Lethaia
AN INTERNATIONAL JOURNAL OF PALAEONTOLOGY AND STRATIGRAPHY

Possible patterns of marine primary productivity during the Great Ordovician Biodiversification Event

ALEXANDRE POHL, DAVID A. T. HARPER, YANNICK DONNADIEU, GUILLAUME LE HIR, ELISE NARDIN AND THOMAS SERVAIS

LETHAIA

Pohl, A., Harper, D.A.T., Donnadieu, Y., Le Hir, G., Nardin, E. & Servais, T. 2017: Possible patterns of marine primary productivity during the Great Ordovician Biodiversification Event. *Lethaia*, https://doi.org/10.1111/let.12247.

Following the appearance of numerous animal phyla during the 'Cambrian Explosion', the 'Great Ordovician Biodiversification Event' (GOBE) records their rapid diversification at the lower taxonomic levels, constituting the most significant rise in biodiversity in Earth's history. Recent studies suggest that the rapid rise in phytoplankton diversity observed at the Cambrian–Ordovician boundary may have profoundly restructured marine trophic chains, paving the way for the subsequent flourishing of plankton-feeding groups during the Ordovician. Unfortunately, the fossil record of plankton is incomplete. Its smaller members represent the bulk of the modern marine biomass, but they are usually not documented in Palaeozoic sediments, preventing any definitive assumption with regard to an eventual correlation between biodiversity and biomass at that time. Here, we use an up-to-date ocean general circulation model with biogeochemical capabilities (MITgcm) to simulate the spatial patterns of marine primary productivity throughout the Ordovician, and we compare the model output with available palaeontological and sedimentological data. ☐ *Climate modelling, GOBE, Ordovician, Palaeoceanography, primary productivity.*

Alexandre Pohl ✉ [pohl@cerege.fr], and Yannick Donnadieu [donnadieu@cerege.fr], Aix Marseille Université, CNRS, IRD, Coll France, CEREGE, Aix-en-Provence, France; David A. T. Harper [david.harper@durham.ac.uk], Palaeoecosystems Group, Department of Earth Sciences, Durham University, Durham DH1 3LE, UK; David A. T. Harper [david.harper@durham.ac.uk], Department of Geology, University of Lund, SE 223 62 Lund, Sweden; Guillaume Le Hir [lehir@ipgp.fr], Institut de Physique du Globe de Paris, Université Paris7-Denis Diderot, 1 rue Jussieu Paris, France; Elise Nardin [elise.nardin@get.obs-mip.fr], UMR5563 Géosciences Environnement Toulouse, Observatoire Midi-Pyrénées, CNRS/UPS/IRD, 14 Avenue Edouard Belin, 31400 Toulouse, France; Thomas Servais [thomas.servais@univ-lille1.fr], Univ. Lille, CNRS, UMR 8198-Evo-Eco-Paleo, F-59000 Lille, France; *manuscript received on 29/03/2017; manuscript accepted on 18/08/2017.*

The 'Great Ordovician Biodiversification Event' (GOBE) was arguably the most important and sustained increase of marine biodiversity in Earth's history (e.g. Sepkoski 1995; Webby 2004; Harper 2006). During the so-called Cambrian explosion most, if not all, animal phyla first appeared in the fossil record. Subsequently, during the Ordovician period, an 'explosion' in diversity at the order, family, genus and species level occurred.

The search for the triggers of this biodiversification is ongoing, but most probably there was no unique cause, but the combined effects of several geological and biological processes that helped generate the GOBE.

During the Ordovician, a unique palaeogeographical scenario existed, with the greatest continental dispersal of the Palaeozoic. High sea levels that were the highest during the Palaeozoic, if not of the entire Phanerozoic, allowed marine waters to cover large epicontinental areas and flooded large tropical shelf areas, enabling diversification (e.g. Servais *et al.* 2009, 2010). The climate was warm, although recent studies indicate a significant, long cooling trend throughout the Ordovician, followed up by an abrupt cooling at the end of the period, triggering the Late Ordovician glacial peak (Trotter *et al.* 2008; Nardin *et al.* 2011; Harper *et al.* 2014).

Also during the Ordovician, important ecological evolutionary changes occurred, beginning with the 'explosion' of the phyto- and zooplankton, leading to the 'Ordovician Plankton Revolution' (Servais *et al.* 2008). The onset of the GOBE is actually, at least partly for the planktonic groups, rooted in the late Cambrian, when most of the planktonic organisms started to diversify rapidly (Servais *et al.* 2016). In this context, Saltzman *et al.* (2011) already considered that during the latest Cambrian, a major increase in atmospheric oxygen concentration (pO_2) had already taken place. The temporal correlation between the Cambrian oxygenation event and the

DOI 10.1111/let.12247

concomitant rise in plankton diversity led Saltzman *et al.* (2011) and Servais *et al.* (2016) to hypothesize that the increase in pO_2 might have triggered the increase of plankton diversity, which may be related to changes in macro- and micronutrient abundances in increasingly oxic marine environments. The higher amount of available nutrients in the oceans possibly triggered the development of pico- and phytoplankton, that is the basis of modern marine trophic chains (Saltzman *et al.* 2011; Servais *et al.* 2016). Logically, the trophic chain was then assembled with additional tiers provided by the suspension-feeding benthos (e.g. brachiopods, bryozoans and corals) and nekton, themselves prey to a range of predators, including the trilobites, with orthoconic cephalopods and fishes at and near the top of the food chain.

Great advances have been made during the last decades concerning palaeogeographical reconstructions for the Early Palaeozoic, including the Ordovician (e.g. Torsvik & Cocks 2013). These more reliable global palaeogeographical reconstructions have allowed the formulation of simple conceptual and more complex numerical models for ancient atmospheric and ocean circulation patterns, or to hypothetically locate upwelling zones (e.g. Wilde 1991; Christiansen & Stouge 1999; Herrmann *et al.* 2004; Pohl *et al.* 2014; Servais *et al.* 2014). More recently, new constraints on the palaeobiogeography of marine living communities were provided by the publication of maps showing much more precisely the ocean surface circulation modelled at various atmospheric CO_2 levels during the Early, Middle and Late Ordovician (Pohl *et al.* 2016b).

The aim of this study was to model possible patterns of biomass production in the Ordovician seas in order to attempt to understand where and how the diversification originated. We use here an ocean–atmosphere general circulation model with biogeochemical capabilities (MITgcm) in order to simulate the changing spatial patterns of marine primary productivity in response to the palaeogeographical evolution through the Ordovician. We subsequently attempt to compare the model output with available palaeontological and sedimentological data.

Ordovician biomass and the sedimentary record

Many palaeontologists have focussed on the analyses of palaeobiodiversity during the Phanerozoic (e.g. Sepkoski *et al.* 1981; Alroy 2010; Harper *et al.* 2015). Such studies led to the understanding of the major trends in biodiversification during Earth history, and to the discovery of the major extinction phases, including the big-five mass extinctions. Specialists in macroevolution and macroecology usually apply various statistical methods in order to better understand and interpret the changing palaeobiodiversities (e.g. Sepkoski 1995; Bambach 2006; Alroy 2010; Stanley 2016). The GOBE has also been recognized based on these studies.

Biodiversity is a measure of the number of biological organisms present at a given moment, but it usually provides no information about the abundance of these organisms, biodiversity not being (at least directly) linked to the biomass produced (Irigoien *et al.* 2004; Finnegan & Droser 2008). Little attention has been paid to the evolution of the biomass in the oceans (e.g. Franck *et al.* 2006; Kallmeyer *et al.* 2012). Martin (2003), for instance, analysed the fossil record of biodiversity in relation to nutrients, productivity and habitat area, whereas Martin *et al.* (2008) investigated the evolution of ocean stoichiometry (nutrient content) in order to understand the biodiversification of the Phanerozoic marine biosphere. In general, the evolution of the abundance of nutrients available in the oceans during the history of the Earth is only poorly known (e.g. Allmon & Martin 2014). As a result, little information is available about biomass or the patterns of primary productivity in ancient oceans, including that during the GOBE.

Payne & Finnegan (2006) considered that during the GOBE, the increase in the complexity of the marine trophic chains and in the efficiency of marine organisms in removing available food, from both the water column and the sediment, appears to account for a secular increase in animal biomass. Based on Martin *et al.* (2008), Servais *et al.* (2016) further considered that the increasing presence of planktonic organisms in the late Cambrian – Early Ordovician must coincide with increasing nutrient supply, increased primary productivity and expanded biomass production that resulted during the initiation of the GOBE with a higher diversity and increased abundance of plankton-feeding groups during the Ordovician. Nowak *et al.* (2015) effectively observed a dramatic increase in diversity of the acritarchs, that is the organic-walled fraction of the phytoplankton, in the late Cambrian – Early Ordovician interval. But do the higher diversities of phytoplanktonic organisms also indicate an increased abundance of phytoplankton and an increased biomass?

Primary productivity in ancient oceans

Ocean productivity largely refers to the production of organic matter by 'phytoplankton' (e.g. Sigman &

Hain 2012). In summary, most of the single-celled phytoplankton are 'photoautotrophs' that use nutrients and light to convert inorganic to organic carbon. They are subsequently consumed by the 'heterotrophs' that include the 'zooplankton', the 'benthos' and the 'nekton'. The most important nutrients necessary for the phytoplankton are nitrogen (N), phosphorus (P), iron (Fe) and silicon (Si), while sunlight is the basic energy source needed. Until recently, it was assumed that the larger parts of the phytoplankton (between 5 and 100 μm in diameter) account for most phytoplankton biomass and productivity. This larger phytoplankton is partly preserved in the fossil record and corresponds in the Palaeozoic to the informal group of the acritarchs. However, recent studies indicate that more than half of the biomass in modern oceans is actually produced by the much smaller fraction (<2 μm in diameter), referred to as the picoplankton (e.g. Buitenhuis *et al.* 2012). Recent estimates indicate that 30% of the modern oceanic biomass is constituted by picoheterotrophs and 25% of picophytoplankton (e.g. Buitenhuis *et al.* 2013; Moriarty & O'Brien 2013). This small fraction is almost entirely unknown from the fossil record, the picoplankton not being observed by palaeopalynologists because it falls out of the range of classical observational methods. However, most recent studies indicate that it is this fraction that is the most diverse in modern oceans (e.g. de Vargas *et al.* 2015).

Thus, our understanding of the fossil record of the base of the trophic chain is highly incomplete in the Ordovician, as only a minor fraction of the phytoplankton is recorded under the informal grouping of, for example, the acritarchs. A key approach, therefore, to an understanding of biomass production in the Early Palaeozoic is the use of numerical models. In the present study, we apply such a model for three different time intervals in the Ordovician to understand, at least tentatively, marine productivity during the GOBE interval. Our analysis specifically focuses on large-scale upwelling systems, which generate high rates of biomass production and leave a distinctive fingerprint in the sedimentary record.

Upwelling systems, hot spots of primary productivity

Modern coastal upwelling zones have been a focus of investigation for a number of years as loci of bioproductivity. Here, benthic and nektonic diversity is influenced by a wide range of environmental factors together with low-oxygen concentrations and biotic interactions such as competition and predation. Upwelling zones promote bioproductivity through the delivery of nutrient-rich deep water onto the shelf, promoting the growth and abundance of phytoplankton. During the GOBE and early stages of the establishment of the Palaeozoic Evolutionary Fauna, communities were dominated by suspension feeders such as the brachiopods, bryozoans and corals and potentially could benefit directly as primary consumers. There is a wealth of biodiversity data available for all the major benthic and nektonic groups (e.g. Webby *et al.* 2004), but there are relatively few regional studies related to specific geographical areas.

Recent studies of some of the key coastal upwelling zones, for example along the Namibian Coast (Eisenbarth & Zettler 2016), associated with the Benguela Current Large Marine Ecosystem (BCLME), together with those on coastal upwelling along the Peru coast (Rosenberg *et al.* 1983), the effects of El Niño on the benthos of the Benguela, California and Humboldt upwelling ecosystems (Arntz *et al.* 2006) and upwelling along the NW Africa coast (Thiel 1982) have established some key properties for these zones. Primary and secondary production is substantial; however, it also generates low-oxygen conditions commonly moving the oxygen minimum zone (OMZ) into shallower-water environments. Biotas are dominated by soft-bodied taxa, and there is a reduced diversity and evenness and fewer calcified forms (Levin 2003). In many cases, assemblages are dominated by pioneer communities populated by opportunistic species forming dense accumulations. Moreover, the poor oxygen conditions encourage the migration of taxa into shallower water, extending too their geographical ranges along the shelf. Organisms are abundant, generating substantial biomass but not necessarily high diversities.

Methods: model description

Ocean, atmosphere and sea ice

We used a coupled ocean–atmosphere–sea ice set-up of the Massachusetts Institute of Technology general circulation model (MITgcm). An isomorphism between ocean and atmosphere dynamics is exploited to allow a single hydrodynamical core to simulate both fluids (Marshall *et al.* 2004). The oceanic and the atmospheric components also share the same cubed-sphere grid with 32 × 32 points per face (cs32), yielding a mean equatorial resolution of 2.8° × 2.8°. The cubed-sphere grid avoids polar singularities resulting from the convergence of the meridians at the poles, thus ensuring that the model

dynamics there is treated with as much fidelity as elsewhere (Adcroft *et al.* 2004).

The oceanic component is an up-to-date, hydrostatic, implicit free-surface, partial step topography ocean general circulation model (Marshall *et al.* 1997a,b). Twenty-eight levels are defined vertically, the thickness of which gradually increases from 10 m at the surface to 1300 m at the bottom. Effects of mesoscale eddies are parameterized as an advective process (Gent & McWilliams 1990) and an isopycnal diffusion (Redi 1982). The non-local K-profile parameterization (KPP) scheme of Large *et al.* (1994) accounts for vertical mixing in the ocean's surface boundary layer, and the interior. The atmospheric physics is based on the simplified parameterizations, primitive equation dynamics (SPEEDY) scheme (Molteni 2003). The latter comprises a four-band long-wave radiation scheme, a parameterization of moist convection, diagnostic clouds and a boundary layer scheme. A low vertical resolution is used. Five levels are defined: one level represents the planetary boundary layer, three layers are placed in the troposphere and the fifth layer is placed in the stratosphere. The pressure coordinate p is employed. Sea ice is simulated using a thermodynamic sea ice model based on the Winton (2000) two-and-a-half-layer enthalpy-conserving scheme. Sea ice growth occurs when the ocean temperature falls below the salinity-dependent freezing point.

Fluxes of momentum, freshwater, heat and salt are exchanged every 20 min in the model (i.e. the ocean time step). The resulting coupled model can be integrated for ca. 100 years in one day of dedicated computer time. Relatively similar model configurations were used in the past (Enderton & Marshall 2009; Ferreira *et al.* 2010, 2011), including those for palaeoceanographical purposes (Brunetti *et al.* 2015; Pohl *et al.* 2017).

Primary productivity

The MITgcm includes a biogeochemistry model that simulates the net primary productivity (NPP) in the ocean. NPP is computed based on Michaelis–Menten equations as a function of available photosynthetically active radiation (PAR) and phosphate concentration (PO_4):

$$\mathrm{NPP} = \alpha \frac{\mathrm{PAR}}{\mathrm{PAR} + K_{\mathrm{PAR}}} \frac{\mathrm{PO_4}}{\mathrm{PO_4} + K_{\mathrm{PO_4}}}$$

where $\alpha = 2 \times 10^{-3}$ mol/m^3/year is the maximum community productivity, $K_{\mathrm{PAR}} = 30$ W/m^2 the half saturation light constant, and $K_{\mathrm{PO_4}} = 5 \times 10^{-4}$ mol/m^3, the half saturation phosphate constant. In this configuration, phosphate is the single limiting nutrient. It is consumed in the photic zone to fuel the marine primary productivity, regenerated by remineralization throughout the water column based on the empirical law of Martin *et al.* (1987), redistributed within the ocean using the velocity and diffusivity fields provided by the general circulation model and ultimately returned back to the ocean surface in upwelling zones. Because phosphate is assumed to have an oceanic residence time much longer than the oceanic turnover time-scale (i.e. 10–40 kyr; Ruttenberg 1993; Wallmann 2003), its global oceanic concentration is fixed in the model (Dutkiewicz *et al.* 2005). Iron is known as another major factor in productivity (Falkowski 2012). Because it is mainly delivered to the ocean surface as dust from deserts, the emissions of which are difficult to quantify today (Bryant 2013), providing the model with seasonal maps of iron input in the Ordovician is challenging. Although our biogeochemical model has the provision to account for cycling of iron, we prefer not to consider iron fertilization here. The PAR is computed at the ocean surface as a fraction of the incident shortwave radiation provided by the atmospheric component of the MITgcm. It is then attenuated throughout the water column assuming a uniform extinction coefficient. Similar configurations of this biogeochemistry model have been used in the past (Friis *et al.* 2006, 2007), including those for the Ordovician (Pohl *et al.* 2017).

Boundary and initial conditions

We ran our model on three palaeogeographical reconstructions representative of the Early Ordovician (480 Ma, Tremadocian), the Middle Ordovician (460 Ma, Darriwilian) and the early Silurian (440 Ma, Aeronian). The location of the continental masses is taken from the reconstructions by Torsvik & Cocks (2009). The topography and the bathymetry are reconstructed based on published global reconstructions, with additional information from regional studies for Gondwana (e.g. Torsvik & Cocks 2013), Laurentia (e.g. Cocks & Torsvik 2011), Baltica (e.g. Cocks & Torsvik 2005), Siberia (e.g. Cocks & Torsvik 2007) and Asia (e.g. Cocks & Torsvik 2013). Because the location and depth of Ordovician ocean ridges are not well constrained, they are not included in the model. We use a flat-bottom ocean, the depth of which is set to present-day mean seafloor depth, that is −4000 m (Pohl *et al.* 2014). The flat bottom is not expected to constitute a major bias. Several studies on Late Palaeozoic oceans suggest that it does not critically impact the large-scale patterns

of simulated ocean circulation (Montenegro *et al.* 2011; Osen *et al.* 2012). The resulting palaeomaps are very similar to those used by Pohl *et al.* (2016b).

A gradual greening of the continents occurred throughout the Ordovician. The first, non-vascular land plants are documented from the Middle Ordovician Dapingian (Rubinstein *et al.* 2010). There is no evidence of plants on land before that date, including during the Tremadocian, that is the first time-slice used in the present study. In addition, the spatial cover of this primitive vegetation is difficult to estimate for the remainder of the period (Edwards *et al.* 2015; Porada *et al.* 2016). As a consequence, we here follow previous studies (Nardin *et al.* 2011; Pohl *et al.* 2014, 2016a) and impose a rocky desert landscape on the continents (ground albedo of 0.24, which is potentially modified by snow).

During the Ordovician, the atmospheric partial pressure of CO_2 (pCO_2) was significantly higher than today (e.g. Berner 2006). However, the MITgcm does not account for varying pCO_2 levels. It is tuned to the present-day pCO_2. We therefore increased the solar forcing in the model to simulate various climatic states (Ferreira *et al.* 2011) and subsequently compared the simulated temperatures with Ordovician estimates. A solar constant of 350 W/m^2 (instead of 342 W/m^2 today) induces an increase in tropical sea-surface temperatures (SSTs) up to 32.5 °C to 33.7 °C (depending on the time-slice considered). These values compare well with the SSTs reconstructed by Trotter *et al.* (2008) for the Middle Ordovician based on $\partial^{18}O$ measurements (see their fig. 3 in particular). Alternative values would better fit the Early and the Late Ordovician SSTs, but we here aim at quantifying the impact of the palaeogeographical changes on the spatial patterns of Ordovician primary productivity, all other things kept equal. We therefore conduct our three simulations using a solar constant of 350 W/m^2, which is here selected to provide the best match with Middle Ordovician SST estimates. The orbital configuration is defined with an obliquity of 23.45° and an eccentricity of 0°.

We use identical initial conditions in all simulations, including a homogeneous salinity of 35 psu (practical salinity units) and a theoretical latitudinal gradient of ocean temperature characterized by equatorial and polar SSTs of respectively 35 °C and 6 °C and an ocean bottom potential temperature of 3 °C. These values ensure that the ocean is sea ice free at the beginning of each model run. Phosphate is initialized with its present-day depth profile. For each simulation, the physical ocean–atmosphere–sea ice model is first run until deep-ocean equilibrium is reached (≥2000 model years). It is subsequently restarted with marine biogeochemistry for 550 additional years and climatic fields used for analysis are averaged over the last 50 years of the simulation.

Results: simulated Ordovician marine productivity

In space: wind belts and Ekman pumping

The main patterns of simulated Ordovician surface primary productivity (Fig. 1) reflect in simple terms the ocean phosphate concentration, while the PAR only imposes a hemispheric-scale decrease of NPP with latitude. The phosphate concentration in surface sea waters results, in turn, from the large-scale patterns of Ekman pumping. The concentration in PO_4 is lower in shallow waters because nutrients are consumed during photosynthesis and it increases with depth due to remineralization of sinking particles. Upwelling systems allow nutrient-rich deep waters to be transported back to the surface and they are therefore associated with locally high phosphate content. Conversely, downwelling areas are poor in nutrients. The spatial patterns of upwelling and downwelling are essentially driven by the direction of the wind blowing over the ocean surface through Ekman pumping and suction. The trade winds induce large-scale upwelling systems on the western margin of tropical landmasses, and the westerlies cause high phosphate concentrations at the mid-latitudes (40°–60°). Between the trade winds and the westerlies, the downwelling of surface waters along the tropics (30°) leads to low phosphate levels. A local minimum in phosphate concentration and thus primary productivity occurs in the Palaeo-Tethys, between the eastern coasts of Baltica and the western margin of tropical Gondwana (Fig. 1A–C). Here, the downwelling of surface waters combines with a strong freshwater input from the continent. The latter results from the intense orographic precipitation that occurs when the moisture-laden westerlies intercept the coastal topography of Gondwana. Pohl *et al.* (2017) demonstrated that this strong run-off to the ocean is a robust model result that it not overly model-dependent. While the polar latitudes (60°–90°) are dynamically isolated from the global ocean and thus depleted in phosphate in the Northern Hemisphere (Pohl *et al.* 2017), deep-water convection along the coast of Gondwana (e.g. Poussart *et al.* 1999; Herrmann *et al.* 2004) drives the local enrichment of surface waters in nutrients, ensuring relatively high productivity levels there.

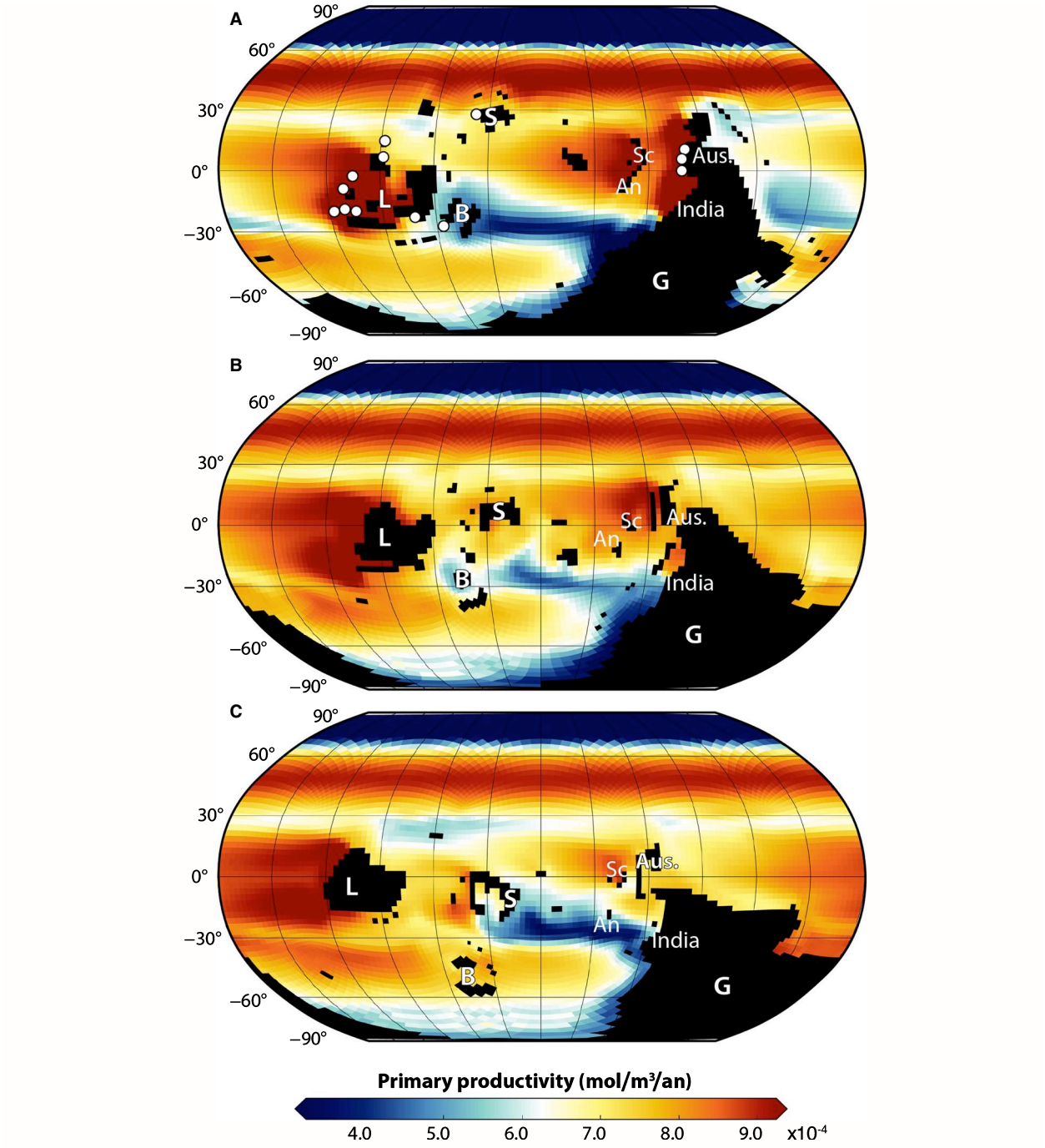

Fig. 1. Surface primary productivity simulated at 440 Ma (A), 460 Ma (B) and 480 Ma (C). The black mask indicates continental masses. In (A), white points represent evidence of upwelling. The latter are plotted on the Late Ordovician time-slice following Pope & Steffen (2003), but see discussion in the main text. *L*: *Laurentia*; *B*: *Baltica*; *S*: *Siberia*; *G*: *Gondwana*; *Sc*: *South China*; *An*: *Annamia*; *Aus*: *Australia*. [Colour figure can be viewed at wileyonlinelibrary.com]

Although the small-scale spatial patterns of simulated NPP may be model-dependent to some extent, the fact that the first-order signal results from a fundamental characteristic of Earth's climate (the zonal wind belts) suggests that these results are relatively robust (Pohl *et al.* 2017).

In time: through the Ordovician

The three studied time-slices share a certain number of common features (Fig. 1). The western margin of Laurentia, first, is associated with high levels of simulated NPP. In both hemispheres, the mid-latitudes

are further characterized by zonal currents inducing Ekman pumping and the upwelling of nutrients fuelling a strong productivity. Conversely, low marine productivity levels typify the tropics (30°), the margin of Gondwana situated over the South Pole and the northern high latitudes. A local minimum persists throughout the period at 30° S between the western coast of Gondwana and the tropical landmasses.

Nevertheless, major changes can be observed from 480 Ma to 440 Ma (Fig. 1). The most considerable alteration of the NPP patterns between the Early and the Late Ordovician resulted from the gradual drift of Gondwana to the North. Confined in the Southern Hemisphere at 480 Ma, the supercontinent reached 30° N at 440 Ma. The direct consequence of this continental drift was the appearance of a major upwelling system at tropical latitudes in the Late Ordovician along the coasts of Gondwana (Australia and India) and South China–Annamia. The contrast between the eastern and western tropical coasts of Gondwana increased at the same time, with simulated NPP significantly decreasing along the eastern coast of Gondwana at 440 Ma. Elsewhere, the spatial patterns of simulated NPP remained relatively stable as the tropical continental masses slowly migrated to the North. This continental drift prompted Siberia to slowly shift, from the Early to the Late Ordovician, from the zone of minimum NPP reported previously at 30° S to the highly productive Panthalassic Circumpolar Current. Conversely, Baltica underwent a migration from nutrient-rich mid-latitude waters in the Southern Hemisphere at 480 Ma to the depleted water masses centred on 30° S at 440 Ma.

Discussion

Here, we compare our modelling results with the Ordovician geological record in order to validate our simulations. We also discuss some enigmatic biotic events in the light of our model runs, such as the sudden and widespread bioherm development that punctuated the Late Ordovician of Baltoscandia.

Geological evidence for upwelling systems

During the Ordovician, two key coastal areas are typified by high levels of primary productivity in the model: the west coasts of Laurentia and tropical Gondwana (Fig. 1), in particular Australia and South China. These modelling results are supported by geological data. Indeed, a wide range of sedimentary indicators has been confirmed for a prolonged phase of upwelling across much of Laurentia during the Middle and Late Ordovician related to glaciation (Pope & Steffen 2003). A careful reassessment of the ages of many of the units (Leslie & Bergström 2003) indicates that the formation of cherts may be much more widespread, suggesting the possibility that this is related to more general phases of upwelling across the Laurentian continent. Associated biotic indicators are sparse and underdeveloped. Graptolites, however, were most common in upwelling zones along continental margins. In the Vinini Formation, Roberts Mountains, Nevada, for example, changes within the graptolite zooplankton have been associated with fluctuating oceanographic conditions and the upwelling of anoxic waters. During high stands, graptolite faunas diversified within the OMZ but the ecosystem collapsed with the substantial fall of sea level associated with the end Ordovician glaciation and the retreat of the OMZ (Finney *et al.* 2007). Elsewhere in the Great Basin, the macro-shelly fauna is abundant throughout much of the Ordovician, locally forming shell beds and concentrations (Finnegan & Droser 2005), with individuals increasing in size (Payne & Finnegan 2006) and shell thickness (Pruss *et al.* 2010); the faunas are never highly diverse, but they are abundant. Bryozoan-rich deposits, formed by another suspension feeder, have also been associated with the upwelling of nutrients in parts of Laurentia during the later Ordovician (Taylor & Sendino 2010).

In detail, the location of the large-scale upwelling systems simulated in the model is in relatively good agreement with most of the evidence of upwelling (cherts and phosphate deposits) documented by Pope & Steffen (2003) (Fig. 1A). Best match is observed on the western margin of the tropical landmasses, that is Laurentia and Gondwana. Some data points are more difficult to explain (e.g. in southeastern Laurentia), and the most outstanding model–data mismatch is observed in Baltica. Clearly, our simulation provides no explanation for the preservation of cherts in that precise location. In order to explain the discrepancy, we emphasize that the spatial resolution of our model (ca. 300 km) does not allow us to capture small-scale processes. In addition, the land–sea mask interpolated on the model's grid constitutes a crude approximation of Ordovician coastlines. Finally, current palaeogeographical reconstructions only provide first-order indications of Early Palaeozoic bathymetry and topography and they generate large uncertainties in the position of the continental masses (up to 15° in latitude) (Lees *et al.* 2002), which makes any straightforward model–data comparison challenging.

To explain the appearance of these unusual carbonates with abundant chert and phosphate, Pope &

Steffen (2003) required the strengthening of the meridional overturning circulation and associated increased nutrient supply to the ocean surface in response to glacial onset during the late Middle Ordovician. Because similarly high levels of primary productivity are simulated on the western margin of Laurentia during each of the three studied time-slices (Fig. 1A–C), with no ice sheet over the South Pole, our model suggests that such coastal upwelling may instead have been a persistent characteristic of Ordovician oceans. These results are supported by the reappraisal of the age of many of the deposits originally reported by Pope & Steffen (2003), a number of them being potentially Early Ordovician in age (Leslie & Bergström 2003). Together, this raises serious doubts about the climatic implications of the phosphatic rocks proposed by Pope & Steffen (2003). Glacial onset does not seem to be a necessary condition for strong upwelling to occur along the margin of Laurentia.

Another possible indicator of high levels of primary productivity is the preservation of sediments enriched in organic matter. Melchin *et al.* (2013) published a compilation of Late Ordovician – early Silurian black shale occurrences. They illustrated three time-slices immediately before, during and right after the Hirnantian glacial peak. Using simulations similar to ours, but focusing on the Late Ordovician, Pohl *et al.* (2017) recently demonstrated a striking correlation between the regions of high/low primary productivity simulated in their model and the preservation of organic-rich/organic-poor sediments in the geological record of the late Katian (i.e. the first time-slice of Melchin *et al.* 2013). Similar to the cherts and phosphate deposits of Pope & Steffen (2003), the black shales are documented on the western margins of equatorial Laurentia and equatorial Gondwana, thus matching simulated upwelling systems (Fig. 1A). More interestingly, the deposits depleted in organic matter are found around Baltica and along the coast of Gondwana over the South Pole (Melchin *et al.* 2013), precisely where the model simulates local NPP minima (Fig. 1A). This model–data agreement supports the spatial patterns of NPP simulated in the present study. It also suggests that the preservation of black shales in the late Katian may have been driven by the patterns of primary production at the ocean surface (Pohl *et al.* 2017).

Baltoscandian reefs and mounds

In their comprehensive review, Kröger *et al.* (2016) demonstrated a critical change in the mode of carbonate production across the Baltic Basin during the latest Sandbian – earliest Katian (Late Ordovician, ca. 453 Ma). This boundary marked the beginning of a protracted period of widespread development of reefs in shallow-water areas and mud mounds in deeper epicontinental settings. The authors showed that biotic factors do not explain the initiation of Late Ordovician bioherm growth. They postulated climatic and eustatic drivers and further identified the northward drift of Baltica as the main determining factor for the timing of the start of the Baltic reef and mound development. More specifically, they suggested that 'the entry of Baltica in a geographical zone that allowed for a widespread bioherm formation was a major factor for the Sandbian radiation of reefal and reef-related organisms'. Although the most direct effect of the latitudinal shift of Baltica was probably the establishment of climatic conditions more favourable to the shallow-water carbonate factory, our model runs also indicate that this northward migration made Baltica enter the nutrient-depleted tropical region during the Late Ordovician (Fig. 1A). Such unparalleled oligotrophic conditions may have provided the appropriate environmental background for the explosion of the bioherms on Baltoscandia.

Limitations

Our simulations provide an overview of possible patterns of Ordovician net primary productivity in time and space. However, it does not tell us anything about the total amount of NPP. The latter is a relatively direct function of nutrient availability in the ocean, which depends in turn on the intensity of continental weathering. Estimating continental weathering requires major assumptions on both the lithology and vegetation cover of emerged continental masses and global climate (e.g. Goddéris *et al.* 2014). In particular, weathering may have significantly varied throughout the Ordovician as a result of changes in global climate (Trotter *et al.* 2008), continental configuration (Nardin *et al.* 2011), volcanic activity (Lefebvre *et al.* 2010), land-ice cover (Pogge von Strandmann *et al.* 2017) or in response to the advent of the first land plants (Lenton *et al.* 2012, 2016; Porada *et al.* 2016). Such mechanisms lie beyond what we are able to resolve using our ocean–atmosphere model. As a result, we are unable to predict the trend towards an increase or a decrease in NPP throughout the period.

Conclusion

Numerical simulations conducted with an ocean–atmosphere general circulation model with

biogeochemical capabilities (MITgcm) predict the position and longevity of upwelling zones in the Ordovician Earth system. Upwelling zones host specific types of ecosystems, characterized by high organic productivity, abundant organisms (commonly opportunistic species, often soft-bodied) but not necessarily high diversities. Nevertheless, high productivity levels may have provided the primary resources needed by superior consumers and thus paved the way for the development of more complex trophic chains featuring more diverse taxonomic assemblages. Fossil data have, to date, not been aligned with these predictions although accumulations of organic matter, bone and skeletal concentrations are identifiable in the fossil record and can be correlated with characteristic sediments, such as cherts, that signpost upwelling zones in deep time. The present study therefore targets in-depth analysis of the smaller members of the fossil record as the logical next step towards the integrated understanding of the diversification patterns throughout the Early Palaeozoic.

Acknowledgements. – The findings of this study are based on climatic fields simulated by the ocean–atmosphere general circulation model MITgcm. Code for the climate model MITgcm can be accessed at http://mitgcm.org. Requests for the climate model output can be sent to A.P. (pohl@cerege.fr). The authors thank Peter Doyle and Alan Owen for editorial handling. We also thank Tom Challands and Axel Munnecke for helpful and constructive reviews, and the guest editors of this volume for the invitation to submit. The authors acknowledge the financial support from the CNRS (INSU, action SYSTER). A.P. and Y.D. thank the CEA/CCRT for providing access to the HPC resources of TGCC under the allocation 2014-012212 made by GENCI. A.P. thanks Maura Brunetti from the University of Geneva and David Ferreira from the University of Reading, who provided expertise that greatly assisted the research. This research was funded through a CEA PhD grant CFR. This is a contribution to the IGCP Project-653, 'The onset of the Great Ordovician Biodiversification Event'. D.A.T.H. acknowledges financial support from the Leverhulme Trust and the Wenner Gren Foundation.

References

Adcroft, A., Campin, J.M. & Hill, C. 2004: Implementation of an atmosphere-ocean general circulation model on the expanded spherical cube. *Monthly Weather Review 132*, 2845–2863.

Allmon, W.D. & Martin, R.E. 2014: Seafood through time revisited: the Phanerozoic increas in marine trophic resources and its macroevolutionary consequences. *Paleobiology 40*, 256–287.

Alroy, J. 2010: The shifting balance of diversity among major marine animal groups. *Science 329*, 1191–1194.

Arntz, W.E., Gallardo, V.A., Gutiérrez, D., Isla, E., Levin, L.A., Mendo, J., Neira, C., Rowe, G.T., Tarazona, J. & Wolff, M. 2006: El Niño and similar perturbation effects on the benthos of the Humboldt, California, and Benguela Current upwelling ecosystems. *Advances in Geosciences 6*, 243–265.

Bambach, R.K. 2006: Phanerozoic biodiversity mass extinctions. *The Annual Review of Earth and Planetary Science 34*, 127–155.

Berner, R.A. 2006: GEOCARBSULF: a combined model for Phanerozoic atmospheric O_2 and CO_2. *Geochimica et Cosmochimica Acta 70*, 5653–5664.

Brunetti, M., Vérard, C. & Baumgartner, P.O. 2015: Modeling the Middle Jurassic ocean circulation. *Journal of Palaeogeography 4*, 371–383.

Bryant, R.G. 2013: Recent advances in our understanding of dust source emission processes. *Progress in Physical Geography 37*, 397–421.

Buitenhuis, E.T., Li, W.K.W., Lomas, M.W., Karl, D.M., Landry, M.R. & Jacquet, S. 2012: Picoheterotroph (Bacteria and Archaea) biomass distribution in the global ocean. *Earth System Science Data 4*, 101–106.

Buitenhuis, E.T., Vogt, M., Moriarty, R., Bednarsek, N., Doney, S.C., Leblanc, K., Le Quérér, C., Luo, Y.-W., O'Brien, C., O'Brien, T., Peloquin, J., Schiebel, R. & Swan, C. 2013: MAREDAT: towards a world atlas of marine ecosystem data. *Earth System Science Data 5*, 227–239.

Christiansen, J.L. & Stouge, S. 1999: Oceanic circulation as an element in palaeogeographical reconstructions: the Arenig (early Ordovician) as an example. *Terra Nova 11*, 73–78.

Cocks, L.R.M. & Torsvik, T.H. 2005: Baltica from the late Precambrian to mid-Palaeozoic times: the gain and loss of a terrane's identity. *Earth-Science Reviews 72*, 39–66.

Cocks, L.R.M. & Torsvik, T.H. 2007: Siberia, the wandering northern terrane, and its changing geography through the Palaeozoic. *Earth-Science Reviews 82*, 29–74.

Cocks, L.R.M. & Torsvik, T.H. 2011: The Palaeozoic geography of Laurentia and western Laurussia: a stable craton with mobile margins. *Earth-Science Reviews 106*, 1–51.

Cocks, L.R.M. & Torsvik, T.H. 2013: The dynamic evolution of the Palaeozoic geography of eastern Asia. *Earth-Science Reviews 117*, 40–79.

Dutkiewicz, S., Follows, M.J. & Parekh, P. 2005: Interactions of the iron and phosphorus cycles: a three-dimensional model study. *Global Biogeochemical Cycles 19*, GB1021.

Edwards, D., Cherns, L. & Raven, J.A. 2015: Could land-based early photosynthesizing ecosystems have bioengineered the planet in mid-Palaeozoic times? *Palaeontology 58*, 803–837.

Eisenbarth, S. & Zettler, M.L. 2016: Diversity of the benthic macrofauna off northern Namibia from the shelf to the deep sea. *Journal of Marine Systems 155*, 1–10.

Enderton, D. & Marshall, J. 2009: Explorations of atmosphere–ocean–ice climates on an aquaplanet and their meridional energy transports. *Journal of the Atmospheric Sciences 66*, 1593–1611.

Falkowski, P. 2012: Ocean science: the power of plankton. *Nature 483*, S17–S20.

Ferreira, D., Marshall, J. & Campin, J.-M. 2010: Localization of deep water formation: role of atmospheric moisture transport and geometrical constraints on ocean circulation. *Journal of Climate 23*, 1456–1476.

Ferreira, D., Marshall, J. & Rose, B. 2011: Climate determinism revisited: multiple equilibria in a complex climate model. *Journal of Climate 24*, 992–1012.

Finnegan, S. & Droser, M.L. 2005: Relative and absolute abundance of trilobites and rhynchonelliform brachiopods across the Lower/Middle Ordovician Boundary, Eastern Basin and Range. *Paleobiology 31*, 480–502.

Finnegan, S. & Droser, M.L. 2008: Body size, energetics, and the Ordovician restructuring of marine ecosystems. *Paleobiology 34*, 342–359.

Finney, S.C., Berry, W.B.N. & Cooper, J.D. 2007: The influence of denitrifying seawater on graptolite extinction and diversification during the Hirnantian (latest Ordovician) mass extinction event. *Lethaia 40*, 281–291.

Franck, S., Bounama, C. & Von Bloh, W. 2006: Causes and timing of future biosphere extinctions. *Biogeosciences 3*, 85–92.

Friis, K., Najjar, R.G., Follows, M.J. & Dutkiewicz, S. 2006: Possible overestimation of shallow-depth calcium carbonate dissolution in the ocean. *Global Biogeochemical Cycles 20*, GB4019.

Friis, K., Najjar, R.G., Follows, M.J., Dutkiewicz, S., Körtzinger, A. & Johnson, M. 2007: Dissolution of calcium carbonate: observations and model results in the subpolar North Atlantic. *Biogeosciences 4*, 205–213.

Gent, P.R. & McWilliams, J.C. 1990: Isopycnal mixing in ocean circulation models. *Journal of Physical Oceanography 20*, 150–155.

Goddéris, Y., Donnadieu, Y., Le Hir, G., Lefebvre, V. & Nardin, E. 2014: The role of palaeogeography in the Phanerozoic history of atmospheric CO_2 and climate. *Earth-Science Reviews 128*, 122–138.

Harper, D.A.T. 2006: The Ordovician biodiversification: setting an agenda for marine life. *Palaeogeography, Palaeoclimatology, Palaeoecology 232*, 148–166.

Harper, D.A.T., Hammarlund, E.U. & Rasmussen, C.M.Ø. 2014: End Ordovician extinctions: a coincidence of causes. *Gondwana Research 25*, 1294–1307.

Harper, D.A.T., Zhan, R.-B. & Jin, J. 2015: The Great Ordovician Biodiversification Event: reviewing two decades of research on diversity's big bang illustrated by mainly brachiopod data. *Palaeoworld 24*, 75–85.

Herrmann, A.D., Haupt, B.J., Patzkowsky, M.E., Seidov, D. & Slingerland, R.L. 2004: Response of Late Ordovician paleoceanography to changes in sea level, continental drift, and atmospheric pCO_2: potential causes for long-term cooling and glaciation. *Palaeogeography, Palaeoclimatology, Palaeoecology 210*, 385–401.

Irigoien, X., Huisman, J. & Harris, R.P. 2004: Global biodiversity patterns of marine phytoplankton and zooplankton. *Nature 429*, 863–867.

Kallmeyer, J., Pockalny, R., Adhikari, R.R., Smith, D.C. & D'Hondt, S. 2012: Global distribution of microbial abundance and biomass in subseafloor sediment. *Proceedings of the National Academy of Sciences of the United States of America 109*, 16213–16216.

Kröger, B., Hints, L. & Lehnert, O. 2016: Ordovician reef and mound evolution: the Baltoscandian picture. *Geological Magazine 154*, 683–706.

Large, W.G., McWilliams, J.C. & Doney, S.C. 1994: Oceanic vertical mixing: a review and a model with a nonlocal boundary layer parameterization. *Reviews of Geophysics 32*, 363–403.

Lees, D.C., Fortey, R.A. & Cocks, L.R.M. 2002: Quantifying paleogeography using biogeography: a test case for the Ordovician and Silurian of Avalonia based on brachiopods and trilobites. *Paleobiology 28*, 343–363.

Lefebvre, V., Servais, T., François, L. & Averbuch, O. 2010: Did a Katian large igneous province trigger the Late Ordovician glaciation? A hypothesis tested with a carbon cycle model. *Palaeogeography, Palaeoclimatology, Palaeoecology 296*, 310–319.

Lenton, T.M., Crouch, M., Johnson, M., Pires, N. & Dolan, L. 2012: First plants cooled the Ordovician. *Nature Geoscience 5*, 86–89.

Lenton, T.M., Dahl, T.W., Daines, S.J., Mills, B.J.W., Ozaki, K., Saltzman, M.R. & Porada, P. 2016: Earliest land plants created modern levels of atmospheric oxygen. *Proceedings of the National Academy of Sciences of the United States of America 113*, 9704–9709.

Leslie, S.A. & Bergström, S.M. 2003: Widespread, prolonged late Middle to Late Ordovician upwelling in North America: a proxy record of glaciation?: comment and reply. *Geology 31*, e28–e29.

Levin, L.A. 2003: Oxygen minimum zone benthos: adaptation and community response to hypoxia. *Oceanography and Marine Biology: An Annual Review 41*, 1–45.

Marshall, J., Adcroft, A., Hill, C., Perelman, L. & Heisey, C. 1997a: A finite-volume, incompressible Navier Stokes model for studies of the ocean on parallel computers. *Journal of Geophysical Research 102*, 5753–5766.

Marshall, J., Hill, C., Perelman, L. & Adcroft, A. 1997b: Hydrostatic, quasi-hydrostatic, and nonhydrostatic ocean modeling. *Journal of Geophysical Research 102*, 5733–5752.

Marshall, J., Adcroft, A., Campin, J.M., Hill, C. & White, A. 2004: Atmosphere-ocean modeling exploiting fluid isomorphisms. *Monthly Weather Review 132*, 2882–2894.

Martin, R.E. 2003: The fossil record of biodiversity: nutrients, productivity, habitat area and differential preservation. *Lethaia 36*, 179–193.

Martin, J.H., Knauer, G.A., Karl, D.M. & Broenkow, W.W. 1987: VERTEX: carbon cycling in the northeast Pacific. *Deep Sea Research 34*, 267–285.

Martin, R.E., Quigg, A. & Podkovyrov, V. 2008: Marine biodiversification in response to evolving phytoplankton stoichiometry. *Palaeogeography, Palaeoclimatology, Palaeoecology 258*, 277–291.

Melchin, M.J., Mitchell, C.E., Holmden, C. & Štorch, P. 2013: Environmental changes in the Late Ordovician-early Silurian: review and new insights from black shales and nitrogen isotopes. *Geological Society of America Bulletin 125*, 1635–1670.

Molteni, F. 2003: Atmospheric simulations using a GCM with simplified physical parametrizations. I: model climatology and variability in multi-decadal experiments. *Climate Dynamics 20*, 175–191.

Montenegro, A., Spence, P., Meissner, K.J., Eby, M., Melchin, M.J. & Johnston, S.T. 2011: Climate simulations of the Permian-Triassic boundary: ocean acidification and the extinction event. *Paleoceanography 26*, PA3207.

Moriarty, R. & O'Brien, T.D. 2013: Distribution of mesozooplankton biomass in the global ocean. *Earth System Science Data 5*, 45–55.

Nardin, E., Goddéris, Y., Donnadieu, Y., Le Hir, G., Blakey, R.C., Pucéat, E. & Aretz, M. 2011: Modeling the early Paleozoic long-term climatic trend. *Geological Society of America Bulletin 123*, 1181–1192.

Nowak, H., Servais, T., Monnet, C., Molyneux, S.G. & Vandenbroucke, T.R.A. 2015: Phytoplankton dynamics from the Cambrian explosion to the onset of the Great Ordovician Biodiversification Event: a review of Cambrian acritarch diversity. *Earth-Science Reviews 151*, 117–131.

Osen, A.K., Winguth, A.M.E., Winguth, C. & Scotese, C.R. 2012: Sensitivity of Late Permian climate to bathymetric features and implications for the mass extinction. *Global and Planetary Change 105*, 171–179.

Payne, J.L. & Finnegan, S. 2006: Controls on marine animal biomass through geological time. *Geobiology 4*, 1–10.

Pogge von Strandmann, P.A.E., Desrochers, A., Murphy, M.J., Finlay, A.J., Selby, D. & Lenton, T.M. 2017: Global climate stabilisation by chemical weathering during the Hirnantian glaciation. *Geochemical Perspectives Letters 3*, 230–237.

Pohl, A., Donnadieu, Y., Le Hir, G., Buoncristiani, J.F. & Vennin, E. 2014: Effect of the Ordovician paleogeography on the (in) stability of the climate. *Climate of the Past 10*, 2053–2066.

Pohl, A., Donnadieu, Y., Le Hir, G., Ladant, J.B., Dumas, C., Alvarez-Solas, J. & Vandenbroucke, T.R.A. 2016a: Glacial onset predated Late Ordovician climate cooling. *Paleoceanography 31*, 800–821.

Pohl, A., Nardin, E., Vandenbroucke, T. & Donnadieu, Y. 2016b: High dependence of Ordovician ocean surface circulation on atmospheric CO_2 levels. *Palaeogeography, Palaeoclimatology, Palaeoecology 458*, 39–51.

Pohl, A., Donnadieu, Y., Le Hir, G. & Ferreira, D. 2017: The climatic significance of Late Ordovician-early Silurian black shales. *Paleoceanography 32*, 397–423.

Pope, M.C. & Steffen, J.B. 2003: Widespread, prolonged late Middle to Late Ordovician upwelling in North America: a proxy record of glaciation? *Geology 31*, 63–66.

Porada, P., Lenton, T.M., Pohl, A., Weber, B., Mander, L., Donnadieu, Y., Beer, C., Pöschl, U. & Kleidon, A. 2016: High potential for weathering and climate effects of non-vascular vegetation in the Late Ordovician. *Nature Communications 7*, 12113.

Poussart, P.F., Weaver, A.J. & Barnes, C.R. 1999: Late Ordovician glaciation under high atmospheric CO_2: a coupled model analysis. *Paleoceanography 14*, 542–558.

Pruss, S.B., Finnegan, S., Fischer, W.W. & Knoll, A.H. 2010: Carbonates in skeleton-poor seas: new insights from Cambrian and Ordovician strata of Laurentia. *Palaios 25*, 73–84.

Redi, M.H. 1982: Oceanic isopycnal mixing by coordinate rotation. *Journal of Physical Oceanography 12*, 1154–1158.

Rosenberg, R., Arntz, W.E., Chuman de Flores, E., Flores, L.A., Carbajal, G., Finger, G. & Tarazona, J. 1983: Benthos biomass and oxygen deficiency in the upwelling system off Peru. *Journal of Marine Research 41*, 263–279.

Rubinstein, C.V., Gerrienne, P., de la Puente, G.S., Astini, R.A. & Steemans, P. 2010: Early Middle Ordovician evidence for land plants in Argentina (eastern Gondwana). *New Phytologist 188*, 365–369.

Ruttenberg, K.C. 1993: Reassessment of the oceanic residence time of phosphorus. *Chemical Geology 107*, 405–409.

Saltzman, M.R., Young, S.A. & Kump, L.R. 2011: Pulse of atmospheric oxygen during the late Cambrian.

Sepkoski Jr, J.J. 1995: The Ordovician Radiations: Diversification and extinction shown by global genus level taxonomic data; pp. 393–396. *In* Cooper, J.D., Droser, M.L. & Finney, S.C. (eds): Ordovician Odyssey: Short Papers, 7th International Symposium on the Ordovician System. Book 77, Pacific Section Society for Sedimentary Geology (SEPM), Fullerton, California.

Sepkoski, J.J., Bambach, R.K., Raup, D.M. & Valentine, J.W. 1981: Phanerozoic marine diversity and the fossil record. *Nature 293*, 435–437.

Servais, T., Lehnert, O., Li, J., Mullins, G.L., Munnecke, A., Nützel, A. & Vecoli, M. 2008: The Ordovician Biodiversification: revolution in the oceanic trophic chain. *Lethaia 41*, 99–109.

Servais, T., Harper, D.A.T., Li, J., Munnecke, A., Owen, A.W. & Sheehan, P.M. 2009: Understanding the Great Ordovician Biodiversification Event (GOBE): influences of paleogeography, paleoclimate, or paleoecology? *GSA Today 19*, 4–10.

Servais, T., Owen, A.W., Harper, D.A.T., Kröger, B. & Munnecke, A. 2010: The Great Ordovician Biodiversification Event (GOBE): the palaeoecological dimension. *Palaeogeography, Palaeoclimatology, Palaeoecology 294*, 99–119.

Servais, T., Danelian, T., Harper, D.A.T. & Munnecke, A. 2014: Possible oceanic circulation patterns, surface water currents and upwelling zones in the Early Palaeozoic. *GFF 136*, 229–233.

Servais, T., Perrier, V., Danelian, T., Klug, C., Martin, R., Munnecke, A., Nowak, H., Nützel, A., Vandenbroucke, T.R.A., Williams, M. & Rasmussen, C.M.Ø. 2016: The onset of the 'Ordovician Plankton Revolution' in the late Cambrian. *Palaeogeography, Palaeoclimatology, Palaeoecology 458*, 12–28.

Sigman, D.M. & Hain, M.P. 2012: The biological productivity of the ocean. *Nature Education 3*, 1–16.

Stanley, S.M. 2016: Estimates of the magnitudes of major marine mass extinctions in earth history. *Proceedings of the National Academy of Sciences 113*, 6325–6334.

Taylor, P.D. & Sendino, C. 2010: Latitudinal distribution of bryozoan-rich sediments in the Ordovician. *Bulletin of Geosciences 85*, 565–572.

Thiel, H. 1982: Zoobenthos of the CINECA area and other upwelling regions. *Rapports et Procès-Verbaux des Réunions du Conseil Permanent International pour l'Exploration de la Mer 180*, 323–334.

Torsvik, T.H. & Cocks, L.R.M. 2009: *BugPlates: linking biogeography and palaeogeography, software manual*. geodynamics.no. Downloaded from http://www.geodynamics.no on 30 July 2014.

Torsvik, T.H. & Cocks, L.R.M. 2013: Gondwana from top to base in space and time. *Gondwana Research 24*, 999–1030.

Trotter, J.A., Williams, I.S., Barnes, C.R., Lécuyer, C. & Nicoll, R.S. 2008: Did cooling oceans trigger Ordovician biodiversification? Evidence from conodont thermometry. *Science 321*, 550–554.

de Vargas, C., Audic, S., Henry, N. *et al.* 2015: Eukaryotic plankton diversity in the sunlit ocean. *Science 348*, 1261605.

Wallmann, K. 2003: Feedbacks between oceanic redox states and marine productivity: a model perspective focused on benthic phosphorus cycling. *Global Biogeochemical Cycles 17*, 1084.

Webby, B.D. 2004: Introduction. *In* Webby, B.D., Paris, F., Droser, M.L. & Percival, I.G. (eds): *The Great Ordovician Biodiversification Event*, 1–37. Columbia University Press, New York.

Webby, B.D., Paris, F., Droser, M.L. & Percival, I.G. (eds) 2004: *The Great Ordovician Biodiversification Event*. Columbia University Press, New York.

Wilde, P. 1991: Oceanography in the Ordovician. *In* Barnes, C.R. & Williams, S.H. (eds): *Advances in Ordovician Geology*, volume 90, 283–298. Geological Survey of Canada, Calgary, Canada.

Winton, M. 2000: A reformulated three-layer sea ice model. *Journal of Atmospheric and Oceanic Technology 17*, 525–531.